

Fig. 2 Membrane stress distribution along $\xi = 0$ for different values of ϵ .

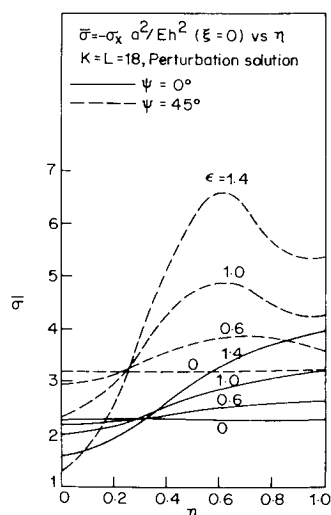


Table 1 Effect of nonlinearity

$\bar{R}_x = \bar{R}_{x \text{ crit}}(1 + K_2 \epsilon^2 + K_4 \epsilon^4 + \dots)$						
ψ	Number of terms in \bar{W} and F $K = L$	$\bar{R}_{x \text{ crit}}$				
		Present note	Ref. 1	Ref. 3	K_2	K_4
0°	9	25.0	26.4	24.9	0.19	-0.03
15°	18	25.8	39.0	25.8	0.20	-0.01
30°	18	28.9	55.8	28.9	0.21	-0.0002
45°	18	35.3	93.0	35.1	0.21	0

the nonlinearity represented mainly by K_2 , coefficient of ϵ^2 , is of a hardening type and tends to remain nearly constant with increasing skew angle.

This also is reflected in the curves of Fig. 1 as they tend to be roughly parallel. In fact, if $\bar{R}_x/\bar{R}_{x \text{ crit}}$ is plotted against the deflection parameter ϵ , the curves for the various skew angles of Fig. 1 of the present Note would be confined to a narrow band unlike the curves of Ref. 1 which indicate that the effect of nonlinearity decreases considerably with increase in skew angle. It may be mentioned here that the near constancy of the magnitude of nonlinearity with skew angle also is depicted in the load vs end shortening plots for different ψ 's which are not presented here for the sake of brevity.

Figure 2 shows the variation of membrane stress σ_x along the center line of the plate for different values of the deflection parameter ϵ for two different skew angles. The magnitude of stress increases with deflection and also with skew angle. For $\psi = 0^\circ$, the location of maximum stress remains on the edge as deflection increases. For $\psi = 45^\circ$, however, the location of maximum stress shifts inwards with increasing deflection. Further, a detailed study of stress distribution for different skew angles shows that this shift increases with skew angle.

References

- Pandalai, K. A. V. and Satyamoorthy, M., "Postbuckling Behavior of Orthotropic Skew Plates," *AIAA Journal*, Vol. 11, No. 5, May 1973, pp. 731-733.
- Leicester, R. H., "Finite Deformations of Shallow Shells," *Proceedings of ASCE, Journal of Engineering Mechanics Division*, Vol. 94, No. EM6, Dec. 1968, pp. 1409-1423.
- Mahabaliraja and Durvasula, S., "Design Data on Buckling of Clamped Skew Plates (Oblique Components), Part—I: Individual Loading," Rept. AE 296 S, May 1971, Dept. of Aeronautical Engineering, Indian Institute of Science, Bangalore, India.

Transition Prediction Technique

J. A. BENEK* AND M. D. HIGH†
ARO, Inc., Arnold Air Force Station, Tenn.

Introduction

ONE of the first boundary-layer transition correlations based upon a theoretical foundation was given by Liepman¹ who hypothesized that laminar breakdown occurred when the ratio of inertial to viscous stresses obtained a critical value. He then used linear stability theory to relate this ratio to flow variables. There have been many subsequent and moderately successful correlation schemes based upon either the Liepman hypothesis or linear stability theory.² The most important in the context of this paper is that of Van Driest and Blumer.³

There have also been numerous experimental investigations of the transition process.⁴⁻⁹ A common feature of these investigations is that the test facility influences the results by introducing either vorticity or acoustic disturbances into the free-stream flow. The manner in which the magnitude of these disturbances varies depends upon the flow regime and test facility. However, the common trend is that as the disturbance magnitude increases, the transition Reynolds number decreases.

Analysis

Liepman's hypothesis can be written as a critical Reynolds number

$$R_{\text{crit}} = (\rho \bar{u}_i \bar{u}_j) / (\mu du/dy)$$

where $\rho \bar{u}_i \bar{u}_j$ is the inertial or Reynolds stress and $\mu du/dy$ is the viscous stress. The critical value, R_{crit} , can be expected to occur somewhere in the interior of the boundary layer, say at $y = y_c$. This expression can be put in a more suitable form for calculation by eliminating $\bar{u}_i \bar{u}_j$ by using the Prandtl mixing length hypothesis, and then by using Pohlhausen's velocity profile to evaluate the velocity gradient. The critical Reynolds number then has the form

$$R_{\text{crit}} = Re_l^2 / [\delta \{F'(\eta_c) + \Lambda G'(\eta_c)\}] \quad (1)$$

where F and G are polynomials in η , $\eta = y/\delta$, δ is the boundary-layer thickness, Re is the unit Reynolds number, l is the mixing length, and Λ for compressible flow is

$$\Lambda = (\rho_\infty/\rho_w)(\delta^2)/(v_\infty \rho_\infty u_\infty)(\partial P/\partial x)$$

where ρ_∞/ρ_w is the ratio of freestream to wall density, v_∞ is the kinematic viscosity, and $\partial P/\partial x$ is the pressure gradient.

The effects of the disturbances can be entered through the pressure gradient, if the pressure is assumed to be linearly composed of a mean pressure, \bar{p} , and two fluctuating pressures, \bar{p}_v and \bar{p}_a where \bar{p}_v is due to vorticity, and \bar{p}_a is due to acoustic disturbances. Further, since the vorticity fluctuations are primarily velocity fluctuations, we can use Taylor's¹⁰ relation $\bar{p}_v \approx \bar{\rho}(\bar{u})^2$ where \bar{u} is the rms velocity fluctuation due to vorticity variations. Thus

$$\Lambda = -\delta^2(\rho_\infty/\rho_w)/v_\infty \rho_\infty u_\infty [\chi \partial \bar{P}/\partial x + F \bar{\rho} \bar{u}^2/\lambda_v + Z \bar{P}_a/\lambda_a]$$

where χ , λ_v , λ_a are appropriate scale lengths. The coefficient $F = (1 + 40M_f)^{1/2}$ (Ref. 11) is a compressibility correction to \bar{p}_v , where $M_f = \bar{u}/u_\infty$. For small fluctuations (i.e., \bar{u} small), $F \approx 1.0$.

Received February 7, 1974; revision received May 28, 1974. The research reported herein was conducted by the Arnold Engineering Development Center, Air Force Systems Command. Research results were obtained by personnel of ARO, Inc., Contract Operator at AEDC. Further reproduction is authorized to satisfy needs of the U.S. Government.

Index category: Boundary-Layer Stability and Transition.

* Research Engineer, 16T/16S Projects Branch, Propulsion Wind Tunnel Facility, Member AIAA.

† Supervisor, 16T/16S Projects Branch, Propulsion Wind Tunnel Facility, Associate Fellow AIAA.

The coefficient Z is the boundary-layer impedance. Following the arguments of Van Driest and Blumer,³ the values of both λ_v and η_c are approximately 0.5 δ . The mixing length l has been taken to be the same order of magnitude as the boundary-layer thickness ($l \approx \delta$). If the laminar boundary-layer thickness is assumed to vary as

$$\delta \approx C(x)^{1/2}/(Re)^{1/2}$$

(Note that this will require $\partial \bar{p}/\partial x \approx 0$.)

The expression for R_{crit} from Eq. (1) becomes

$$R_{crit} = C(Re X_t)^{1/2} [1 + 0.1C(T_w/T_\infty)(Re X_t)^{1/2} \Sigma] \quad (2)$$

where

$$\Sigma = \frac{1}{\lambda_v} [(Z/2)(\lambda_v/\lambda_d) \Delta C_p + (\bar{u}/u_\infty)^2]$$

The behavior of Eq. (2) as Σ approaches zero indicates that $Re X_t$ approaches a constant, $k_1 \equiv (R_{crit}/C)^2$. Using this relation to eliminate R_{crit} in Eq. (2) and then squaring yields a quadric form for $Re X_t$. If terms of $O(\Sigma^2)$ are neglected compared to unity, this relation is

$$(Re X_t)^2 - \{2k_1 + [k_1 k_2 (T_w/T_\infty) \Sigma]^2\} Re X_t + k_1^2 = 0 \quad (3)$$

where

$$k_2 = 0.1C(2)^{1/2}$$

Values of the Constants

Equation (3) can be used to calculate the transition Reynolds number if the value of all the constants is specified. An estimate of the value of λ_v/λ_d can be obtained by considering that those wavelengths that can most effectively disrupt the boundary layer are those which impress a shear on the entire layer. This would imply $\lambda_d \gg \delta$; and therefore, $\lambda_v/\lambda_d \ll 1.0$. By assuming $\lambda_v \approx 0.5\delta$ and using the most amplified frequency from the linear compressible, stability analysis at $M_\infty = 0.8$, the ratio λ_v/λ_d is approximately 0.01. The boundary-layer impedance Z will be taken as unity since the boundary-layer disturbance interaction is poorly understood. The value of C corrected for axisymmetric flow is 1.67.

Equation (3) indicates that for small Σ

$$Re X_t \sim T_w/T_\infty \Sigma$$

Figure 1 is a plot of available data from the AEDC 10° cone⁷⁻⁹ for small values of $(T_w/T_\infty) \Delta C_p$. The $\Sigma = 0$ intercept ($Re X_t = K_1$) obtained by extrapolation is approximately 3×10^6 .

Comparison with Experiment

Since most of the data available to the authors was in the form of beginning of transition location, Eq. (3) was rearranged to the form

$$(X_t/l)^2 - [2k_1/Re + (K_1 K_2/Re)(T_w/T_\infty) \Sigma^2] X_t/l + (K_1/Re)^2 = 0$$

$$K_1 = k_1/l, \quad K_2 = k_2, \quad l = 0.1C 2l \quad (4)$$

where $O(\Sigma^2)$ terms have been neglected compared to unity. The constants K_1 and K_2 have been altered to allow ΔC_p to be entered in percent and Re to be entered in millions per foot.

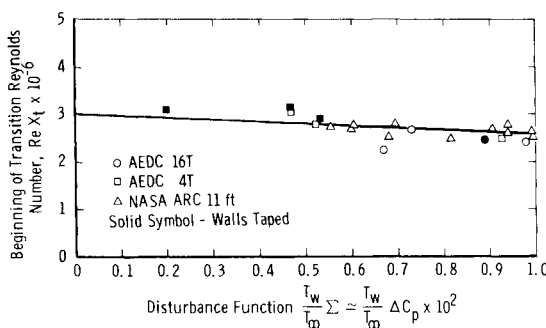


Fig. 1 Transition Reynolds number variation with disturbance function.

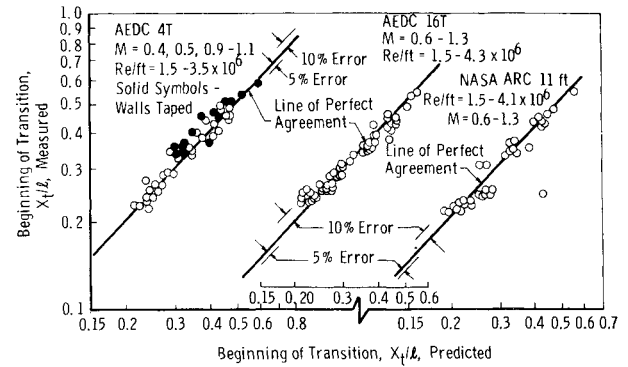


Fig. 2 Comparison of measured and predicted transition locations in several flow facilities.

The values of the constants used for the AEDC 10° cone are $l = 3.0$ ft, $K_1 = 1.0$, and $K_2 = 0.0658$. This latter value was obtained as an optimum from a curve fit of the AEDC 16T Tunnel data and is held constant for the remaining data. However, if the complete equation is used [i.e., retain all $O(\Sigma^2)$ terms], then $K_2 = 0.0408$ as given in Eq. (4). The larger value of K_2 corresponds to the effect of the neglected terms. It is felt that the simpler form of Eq. (4) warrants the neglect of the $O(\Sigma^2)$ terms compared to unity since the larger value of K_2 appears to compensate adequately for their effect.

The following comparison is limited to beginning of transition data obtained from pitot pressure traverses and its definition is taken to be the same as that used in Ref. 4. A considerable body of data documenting transition points defined in other ways or using other techniques is available in the literature but these results have not been shown to be equivalent and thus only the pitot data are given here for comparison.

Transonic Flow Regime

A considerable body of transition data on a 3 ft, 10° included-angle cone has been accumulated by AEDC personnel (not all of which has been published at the time of this writing). These studies include extensive data from the AEDC PWT 16-ft and 4-ft Transonic Wind Tunnels as well as a number of other flow facilities throughout the United States. Therefore, a range of tunnel sizes, geometries, and test section relief techniques (i.e., slots, porous walls, etc.) was available for comparison.

Comparisons of the predicted transition location with the measured locations are shown in Fig. 2. The rms acoustic measurements used in the calculations were taken from one of two cone-mounted microphones located 18 and 26 in. behind the cone apex. It was assumed that these measurements were representative of the acoustic environment of the cone when there was a laminar boundary layer over the microphone.¹³ When transition occurred over the forward microphone, the aft measurements were used, although the boundary layer there was

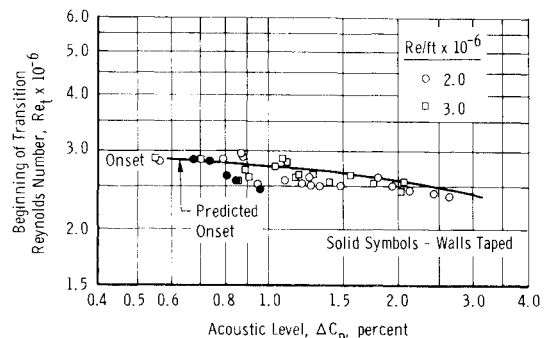


Fig. 3 Transition Reynolds number as a function of acoustic level in the AEDC 16T. Comparison with prediction.

turbulent. It was assumed that in this case, the aft microphone gave a more realistic representation of the acoustic environment. In addition, it was assumed that the disturbance function Σ was comprised solely of acoustic disturbances. A plot of transition data obtained in the AEDC 16T as a function of acoustic level is shown in Fig. 3. The theoretical line was calculated for a Mach number of 0.8. Since the range of Mach numbers is small (0.3–1.6) and since the effect of Mach number is small for this range, this line represents a "mean" prediction line.

Figures 2 and 3 indicate that transition can be predicted to within 10% with reasonable consistency. Additional factors having a significant effect on the data which are not included in the model and/or whose effect could not be removed from the data are: 1) pitch and yaw misalignment; and 2) acoustic levels due to proximity of transition to microphone location.

The present technique has been applied to the low subsonic and supersonic flow regimes for the data of Refs. 4–6 and of 12 and 13. The preliminary results indicate that an extension to these flow regimes is feasible.

Conclusions

The consistency of the preceding results shows that the proposed technique for the prediction of beginning of transition location is justified, at least for 10° included-angle cones. Extension of this method to geometries involving strong pressure gradients may well await a more detailed understanding of the transition process. Therefore, the present work is not presented as a final solution but merely as a useful tool to be used in lieu of exact analysis. The following conclusions can be drawn from the present study. 1) Beginning of transition on 10° included-angle cones can be predicted to within 10%. 2) The technique appears to be extendible to supersonic and low subsonic flow regimes. 3) Noise appears to be at least as important as vorticity in causing transition and in many cases is more important.

References

- Liepmann, H. W., "Investigation of Boundary-Layer Transition on Concave Walls," ARC 4J28, 1945, NACA.
- Hairston, D. E., "Survey and Evaluation of Current Boundary-Layer Transition Prediction Techniques," AIAA Paper 71-985, Washington, D.C., 1971.
- Van Driest, E. R. and Blumer, C. B., "Boundary-Layer Transition: Free Stream Turbulence and Pressure Gradient Effects," *AIAA Journal*, Vol. 1, No. 6, June 1963, pp. 1303–1307.
- Schubauer, G. B. and Skramstad, H. F., "Laminar Boundary-Layer Oscillations and Transition on a Flat Plate," Rept. 909, 1948, NACA.
- Wells, C. S., Jr., "Effects of Freestream Turbulence on Boundary-Layer Transition," *AIAA Journal*, Vol. 5, No. 1, Jan. 1967, pp. 172–175.
- Pate, S. R., "Measurements and Correlations of Transition Reynolds Number on Sharp Slender Cones at High Speed," AEDC-TR-69-172, Dec. 1969, Arnold Engineering Development Center, Tullahoma, Tenn.
- Credle, O. P., "An Evaluation of the Fluctuating Airframe Environment in the AEDC-PWT 4-ft Transonic Tunnel," AEDC-TR-69-236, Nov. 1969, Arnold Engineering Development Center, Tullahoma, Tenn.
- Credle, O. P. and Carleton, W. E., "Determination of Transition Reynolds Numbers in the Transonic Mach Number Range," AEDC-TR-70-218, Oct. 1970, Arnold Engineering Development Center, Tullahoma, Tenn.
- Credle, O. P. and Shadow, T. O., "Evaluation of the Overall Root-Mean-Square Fluctuating Pressure Levels in AEDC PWT 16-ft Transonic Tunnel," AEDC-TR-70-7, Feb. 1970, Arnold Engineering Development Center, Tullahoma, Tenn.
- Taylor, G. I., "Statistical Theory of Turbulence, Part V," *Proceedings of the Royal Society (London)*, Vol. A156, 1936, pp. 307–317.
- Hinze, J. O., *Turbulence: An Introduction to Its Mechanism and Theory*, McGraw-Hill, New York, 1959.
- Palko, R. L., Burt, R. H., and Ray, A. D., "An Experimental Investigation of Boundary-Layer Transition on Flat Plates at Mach Numbers 5, 8, and 10," AEDC-TDR-64-167, Aug. 1964, Arnold Engineering Development Center, Tullahoma, Tenn.

¹³ Benek, J. A. and High, M. D., "A Method for the Prediction of the Effects of Free-Stream Disturbances on Boundary-Layer Transition," AEDC-TR-73-158, Oct. 1973, Arnold Engineering Development Center, Tullahoma, Tenn.

Note on Unsteady Boundary-Layer Separation

JAMES C. WILLIAMS III* AND W. DONALD JOHNSON†
North Carolina State University, Raleigh, N.C.

Nomenclature

A, B	= constants
f	= dimensionless stream function
t	= time
u	= x component of velocity
u_δ	= velocity at upper edge of boundary layer
U	= velocity of moving coordinate system
U_∞	= uniform "freestream" velocity
v	= y component of velocity
x	= physical coordinate parallel to body surface
x_s	= location of the separation point
y	= physical coordinate normal to body surface
η	= dimensionless coordinate normal to body surface
ν	= kinematic viscosity
ξ	= dimensionless coordinate parallel to body surface
ψ	= stream function

Superscript

"—" = overbars denote quantities in moving coordinate system

Introduction

It was recognized quite early that the vanishing of the shear at the wall, which has been such a useful criterion for steady boundary-layer separation, cannot be taken as representing unsteady boundary-layer separation.^{1–3} Moore,¹ Rott,⁴ and Sears⁵ have formulated a model for unsteady separation; a model in which the unsteady separation point is characterized by the vanishing of both the velocity and the shear at some point in the boundary layer "... in a flow seen by an observer moving with the separation point."³ Moore¹ and Sears and Telonis⁵ also argue that this separation point is characterized by a singularity in the solution to the boundary-layer equations.

In the development of this model for unsteady separation both Moore¹ and Telonis⁶ noted a relationship between unsteady boundary layers and steady boundary layers over a moving wall. Moore presented intuitive arguments to relate unsteady separation to steady separation over a moving wall and, on the basis of these arguments, concluded that "a criterion of simultaneous vanishing of shear and velocity is the proper generalization of the usual definition of steady separation, for the case of a separation point moving slowly along a surface." Telonis, also recognized the relation between unsteady separation and steady separation over a moving wall and further showed that a given flow over a moving wall can be transformed into an equivalent unsteady problem by a simple transformation. The analysis of Telonis involved only a transformation of velocities, however,

Received February 8, 1974; revision received April 4, 1974. This work was supported by the U.S. Army Research Office—Durham under Grant DA-ARO-D-31-124-72-G134.

Index categories: Boundary Layers and Convective Heat Transfer—Laminar; Nonsteady Aerodynamics.

* Professor and Associate Head, Department of Mechanical and Aerospace Engineering, Associate Fellow AIAA.

† Graduate Research Assistant, Department of Mechanical and Aerospace Engineering, Member AIAA.